GEOS 657 – MICROWAVE REMOTE SENSING

GRADUATE-LEVEL COURSE AT THE UNIVERSITY OF ALASKA FAIRBANKS

Lecturer:
Franz J Meyer, Geophysical Institute, University of Alaska Fairbanks, Fairbanks; fjmeyer@alaska.edu

Lecture 11: Concepts of Polarimetric SAR

UAF Course GEOS 657

REHASHING POLARIMETRIC SIGNALS

Polarization States of a Coherent Plane Wave

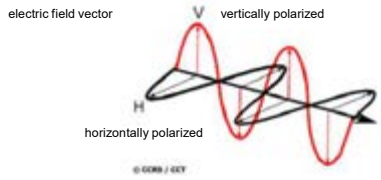

Linearly Polarized Signals

- **Several stages of linear polarization possible**
  - Horizontal polarization (a)
  - Vertical polarization (b)
  - Linear -45º polarization (c)
  - Linear +45º polarization (d)

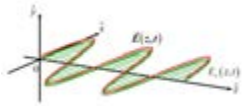

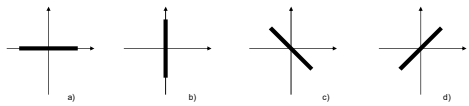

Circular and Elliptical Polarization

- **Combination of vertically and horizontally polarized signals**
  - Right circular polarization (a)
  - Left circular polarization (b)
  - Right elliptical polarization (c)
  - Left elliptical polarization (d)

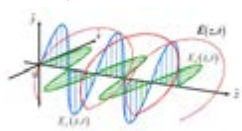

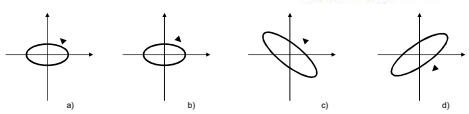

Polarization of SAR Systems

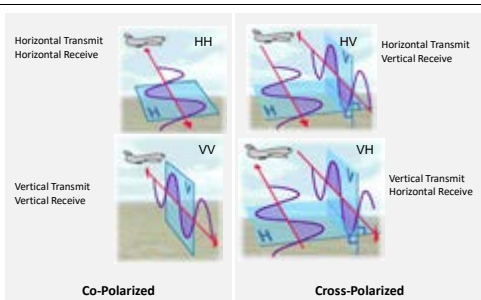

Polarimetric SAR System Configurations

- **single pol:**
  - VV or HH (or possibly HV or VH)
- **dual pol:**
  - HH and HV, VV and VH, or HH and VV
- **quad pol (fully polarimetric):**
  - HH, VV, HV, and VH

relative phase between channels is important information

Scheme of a Dual-Pol System

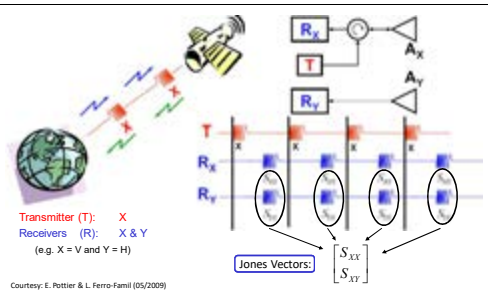

Courtesy: E. Pottier & L. Ferro-Famil (05/2009)

Scheme of a Quad-Pol System

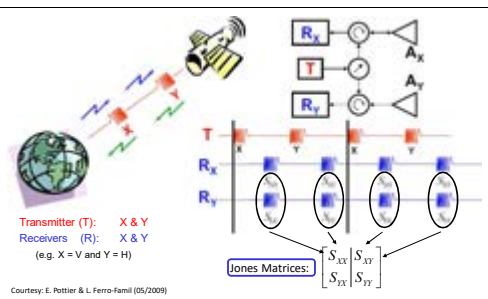

Courtesy: E. Pottier & L. Ferro-Famil (05/2009)

Polarimetric Scattering Matrix

In a quad-pol SAR, every pixel is represented by a matrix of four complex numbers, representing ratios of received and transmitted electric-field amplitudes:

$$[S] = \begin{pmatrix} S_{HH} & S_{HV} \\ S_{VH} & S_{VV} \end{pmatrix} \quad \text{(scattering or Jones matrix)}$$

For (monostatic) SARs: $S_{VH} = S_{HV}$ (reciprocity)

$$[S] = \begin{pmatrix} S_{HH} & S_{HV} \\ S_{HV} & S_{VV} \end{pmatrix} \quad \text{(Sinclair matrix)}$$

$\Rightarrow$ 3 amplitudes + 2 independent phases per pixel

INTERPRETATION OF POLARIMETRIC SAR DATA

To Make Sense of Polarization, It Is Convenient to Assume that the World is Made Up of Three Different Types of Targets

- **Radar scattering is physical and can be described as a series of bounces on scattering interfaces**
- **Three main scattering mechanisms dominate**:
  - **Scattering on (rough) surfaces**: Water, bare soils, roads – Scattering strongly dependent on surface roughness and sensor wavelength
  - **Double-bounce scattering**: Buildings, tree trunks, light poles – little wavelength dependence
  - **Volume Scattering**: Vegetation; dry soils with high penetration – strongly dependent on sensor wavelength and dielectric properties of medium

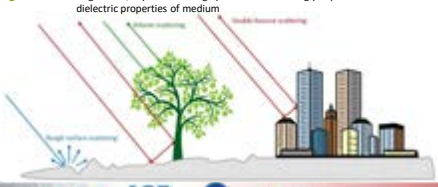

Scattering Processes: Rough Surface (Bragg) Scattering

- **Polarimetric Dependence of Bragg scattering:**
  - Horizontal polarization:
    $$R_{HH} = m \cdot \frac{cos\theta_i - \sqrt{\varepsilon_r - sin^2\theta_i}}{cos\theta_i + \sqrt{\varepsilon_r - sin^2\theta_i}}$$
  - Vertical polarization:
    $$R_{VV} = m \cdot \frac{(\varepsilon_r - 1)[sin^2\theta_i - \varepsilon_r(1 + sin^2\theta_i)]}{\left(\varepsilon_r \cdot cos\theta_i + \sqrt{\varepsilon_r - sin^2\theta_i}\right)^2}$$
  - Cross polarizations:
    $$R_{HV} = R_{VH} = 0$$

... where e is the dielectric constant of the surface and *m* depends on surface roughness

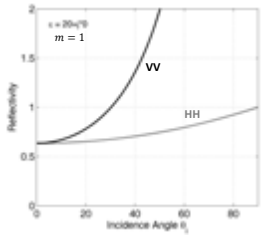

➢ **Scattering Matrix:** $[S] = m\begin{bmatrix} R_{HH} & 0 \\ 0 & R_{VV} \end{bmatrix}$

Scattering Processes: Fresnel Reflection

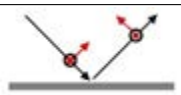

Scattering Matrix: $[S] = \begin{bmatrix} R_H & 0 \\ 0 & R_V \end{bmatrix}$

Fresnel Reflection Coefficients:

$$R_H = \frac{\cos\theta - \sqrt{\varepsilon - \sin^2\theta}}{\cos\theta + \sqrt{\varepsilon - \sin^2\theta}} \quad \text{and} \quad R_V = \frac{\varepsilon\cos\theta - \sqrt{\varepsilon - \sin^2\theta}}{\varepsilon\cos\theta + \sqrt{\varepsilon - \sin^2\theta}}$$

... where ε is the dielectric constant of the surface

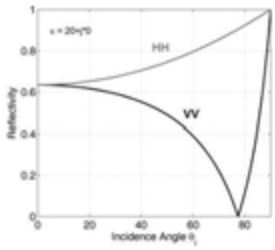

This explains direct reflection off smooth surfaces

Scattering Processes: Fresnel Reflection

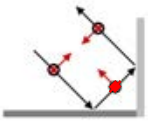

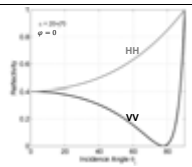

Scattering Matrix:

$$[S] = \begin{bmatrix} 1 & 0 \\ 0 & -1 \end{bmatrix} \begin{bmatrix} 1 & 0 \\ 0 & e^{i\varphi} \end{bmatrix} \begin{bmatrix} R_{SS} & 0 \\ 0 & R_{PS} \end{bmatrix} \begin{bmatrix} R_{ST} & 0 \\ 0 & R_{PT} \end{bmatrix} = \begin{bmatrix} R_{SS}R_{ST} & 0 \\ 0 & -R_{PS}R_{PT}e^{i\varphi} \end{bmatrix}$$

Fresnel Coefficients:

$$R_{SS} = \frac{\cos\theta - \sqrt{\varepsilon_S - \sin^2\theta}}{\cos\theta + \sqrt{\varepsilon_S - \sin^2\theta}} \quad \text{and} \quad R_{PS} = \frac{\varepsilon_S\cos\theta - \sqrt{\varepsilon_S - \sin^2\theta}}{\varepsilon_S\cos\theta + \sqrt{\varepsilon_S - \sin^2\theta}}$$

$$R_{ST} = \frac{\cos\theta - \sqrt{\varepsilon_T - \sin^2\theta}}{\cos\theta + \sqrt{\varepsilon_T - \sin^2\theta}} \quad \text{and} \quad R_{PT} = \frac{\varepsilon_T\cos\theta - \sqrt{\varepsilon_T - \sin^2\theta}}{\varepsilon_T\cos\theta + \sqrt{\varepsilon_T - \sin^2\theta}}$$

Courtesy: I. Hajnsek/DLR

Polarimetric Dependence of Scattering Principles

Relative scattering strength by polarization:

- **Pure Surface Scattering:** $|S_{VV}| > |S_{HH}| > |S_{HV}|$ *or* $|S_{VH}|$
- **Double Bounce Scattering:** $|S_{HH}| > |S_{VV}| > |S_{HV}|$ *or* $|S_{VH}|$
- **Volume Scattering:** main source of $|S_{HV}|$ *and* $|S_{VH}|$

Legend

Low Radar Brightness ($|S|$) High Radar Brightness ($|S|$)

Visual Interpretation

- **Simplest method for classifying polarimetric imagery**
- **Present data in a color image to support interpretation**
- **Suggested "realistic looking" color assignment:**
  - HH = red HV = green VV = blue
  - Water reflections have high VV
  - Vegetation has higher than average HV

Think – Pair – Share

- **Color composite of an ALOS PALSAR (L-band) scene over Washington, DC**
- The following color coding was applied

$$\vec{s} = \begin{bmatrix} S_{HH} \\ S_{HV} + S_{VH} \\ S_{VV} \end{bmatrix}$$

- **[Q1]:** What are the red areas in this image?
- **[Q2]:** What may cause this region to appear white?
- **[Q3]:** This is a river. Why is does it appear in a purple color rather than blue?

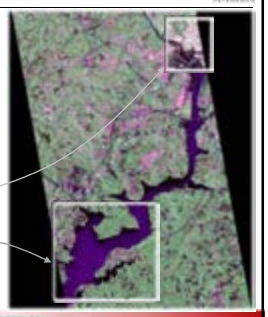

Sinclair Decomposition

- **Definition**:
  - $\vec{s} = \begin{bmatrix} S_{HH} \\ S_{HV} + S_{VH} \\ S_{VV} \end{bmatrix}$ Double bounce dominated / Volume dominated / Surface dominated
- **Example**:
  - ALOS PALSAR (L-band) data over Washington, D.C.

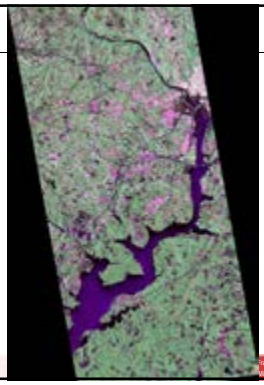

Example of Multiple Polarizations for Vegetation Studies - Pacaya-Samiria Forest Reserve in Peru

- L-band SAR images from UAVSAR (HH, HV, VV)

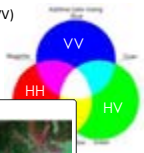

RGB Combination of Polarizations

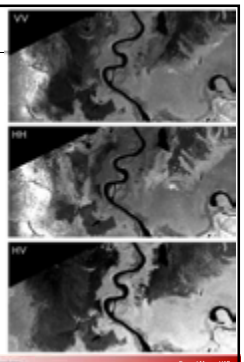

SAR Signatures of Vegetation at Various Frequencies and Polarizations

Increase of penetration depth with wavelength

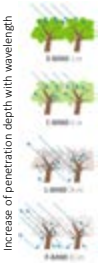

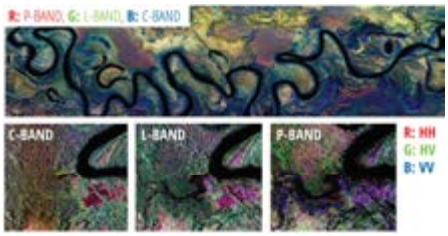

Polarimetric signature change and sub-canopy features are exposed as wavelength increases

SAR Handbook: Comprehensive Methodologies for Forest Monitoring and Biomass Estimation. Eds. Flores, A., Herndon, K., Thapa, R., Cherrington, E. NASA. 2019. DOI: 10.25966/hbm1-ej07

Polarimetric Signatures of Different Types of Agricultural Crops

- **The structure of Crops/vegetation defines scattering power at different polarizations:**
  - Voluminous leafy vegetation will scatter strongly in HV
  - Stemmy vegetation (e.g., corn) will dominate in HH
  - Bare fields and low vegetation stronger in VV

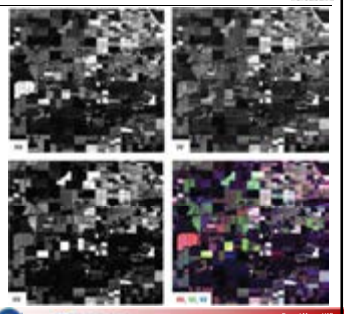

Example:
JPL UAVSAR image acquired by L-band radar showing three backscatter polarizations and the false-colored composites over an area in California's Central Valley covered by orchards and different crops. The strength of each polarized backscatter is shown, relatively suggesting how certain crops are relatively higher in one of the HH, HV, and VV polarizations.

Different Ways Of Representing Polarimetric Data

- **Commonly used polarimetric target descriptors include:**
  - [S] Sinclair matrix
  - $\underline{k}$ Pauli Scattering Vector
  - [K] Kennaugh Matrix
  - [T] Coherency Matrix
  - [C] Covariance Matrix

Will not be discussed here

- Pauli Vector, Kennaugh matrix, and Coherency matrix are closely related to physical properties of the scatter → allow insight into surface structure
- Sinclair Matrix and Covariance matrix are directly related to the system measurables

The Pauli Scattering Vector

- The Scattering matrix can be decomposed by a set of "Pauli Matrices" Ψ_P resulting in the Pauli vector $\underline{k}$

$$\underline{k} = \frac{1}{2} trace([S][\Psi_P])$$

where

$$[\Psi_P] = \left\{ \sqrt{2}\begin{bmatrix} 1 & 0 \\ 0 & 1 \end{bmatrix}, \sqrt{2}\begin{bmatrix} 1 & 0 \\ 0 & -1 \end{bmatrix}, \sqrt{2}\begin{bmatrix} 0 & 1 \\ 1 & 0 \end{bmatrix}, \sqrt{2}\begin{bmatrix} 0 & -j \\ j & 0 \end{bmatrix} \right\}$$

- Resulting in:

$$\underline{k} = \frac{1}{\sqrt{2}} \left[S_{HH} + S_{VV} \quad S_{HH} - S_{VV} \quad S_{HV} + S_{VH} \quad j(S_{HV} - S_{VH}) \right]^T$$

Surface scattering | Double bounce scattering | Volume scattering

⇨ Related to physical properties of the scatterers

The Pauli Scattering Vector

- **In the monostatic case (where you can assume that HV = VH) the Pauli Vector reduces to three elements:**

$$\underline{k} = \frac{1}{\sqrt{2}} \begin{bmatrix} S_{HH} + S_{VV} \\ S_{HH} - S_{VV} \\ 2S_{HV} \end{bmatrix}$$

Surface scattering
Double bounce scattering
Volume scattering

- It makes sense to represent these parameters in an RGB image with red = double bounce, green = volume scattering, and blue = single bounce

The Pauli Vector – A Polarimetric Decomposition

- **Technically speaking, the Pauli Vector is a "Polarimetric Decomposition":**
  - Take a complex matrix of correlated parameters
  - Decompose into sum of (orthogonal) component matrices, each of which has some simpler physical interpretation
- **Typical Decomposition Techniques include:**
  - Cholesky decomposition
  - Eigendecomposition
  - Singular Value Decomposition
  - Pauli Decomposition
  - …
- **Goals:** Decompose complex correlated measurements into uncorrelated components that are easier to interpret

Pauli & Sinclair Decomposition

Washington, D.C., Example

Pauli decomposition (HH-VV, HV+VH, HH+VV)
(even bounce, volume, odd bounce)

Sinclair decomposition (HH, HV+VH, VV)
(*preferred* double bounce, volume, *preferred* surface)

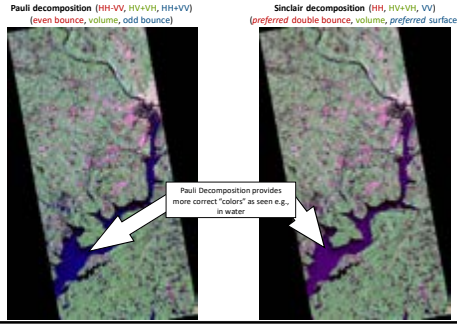

27

Visual Interpretation – Color Composites

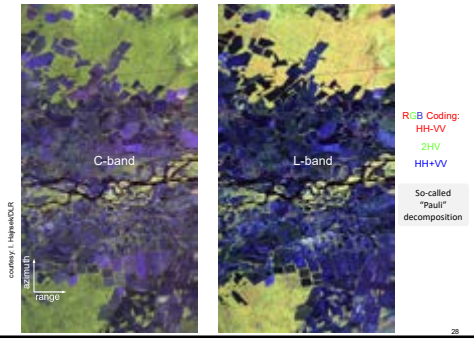

28

Scene Classification based on Polarimetric Decompositions

- **Unsupervised classifiers have been introduced in the recent years**
  - Based on physical properties of target and dominant scattering mechanism and NOT on dataset
    → No prior knowledge about scene content or terrain classes necessary
- **Main decomposition-based classifiers:**
  - Van Zyl: "odd bounce," "even bounce," "diffuse"
  - Freeman: Three component scattering model based classification
  - Cloude & Pottier: H / α Classifier
  - Cloude & Pottier: H / A / α Classifier
  - Yamaguchi: Four Component scattering model based classification (extension of Freeman)
- **Newest methods combine unsupervised methods (e.g., H / A) with a subsequent supervised classifier to improve results**

The Unsupervised H / α Classifier

- **Eigendecomposition** of the coherency matrix (i.e., reduction large number of parameters into an orthogonal set of parameters that contain meaningful information) → Physical interpretation of Eigenvalues
  - **Polarimetric Entropy (H)** [calculated from ratio of Eigenvalues]:
    - Represents *randomness* of scattering with H = 0 indicates single scattering mechanism and H = 1 represents random mix of mechanisms

  - **The (average) $\bar{\alpha}$ Angle** [calculated from Eigenvector]: Indicative of dominant scattering mechanism
    - If $\bar{\alpha} \approx 0^{\circ}$ → surface scattering
    - If $\bar{\alpha} \approx 45^{\circ}$ → volume scattering
    - If $\bar{\alpha} \approx 90^{\circ}$ → dihedral or multiple scattering

$$\bar{\alpha} = \sum_{i=1}^{3} \alpha_i P_i$$

with $P_i = \frac{\lambda_i}{\lambda_1+\lambda_2+\lambda_3}$

and α_i = angle relative to vertical

The Unsupervised H / α Classifier

- **The H/α diagram is shown below**
- By definition, all image pixels will have H/α values within the feasible region

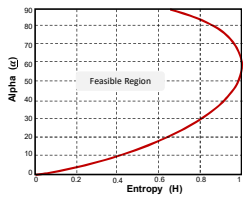

Example of SAR Data in H / α Diagram

- **TerraSAR-X SAR Data**
- **Agricultural Fields are shown**
- **Data Characteristics:**
  - Spread across a range of H values with average of $H \approx 0.8$
  - Low α indicates dominance of surface scattering
  - Indications of variations of crop density on fields

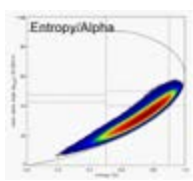

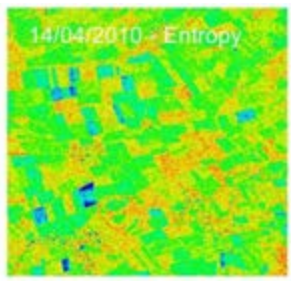

The Unsupervised H / α Classifier

- **The H/α plane is partitioned into nine classes**
- Classes are chose on general properties of scattering

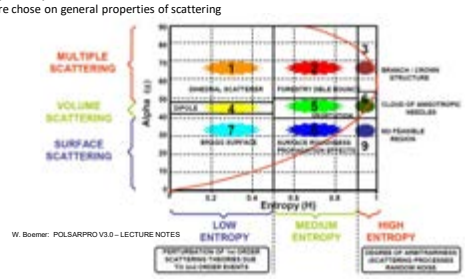

W. Boemer: POLSARPRO V3.0 – LECTURE NOTES

Refinement: The Unsupervised H / A / α (Entropy/Anisotrophy/Alpha) Classifier

- In cases of high Entropy (H > 0.7), the H / α classification scheme is not unique.
- E.g. we can not discriminate between the following scattering cases:

- **Anisotrophy** was introduced to solve these problems by distinguishing cases where l2 ≈ l3 from cases where l2 is large and l3 is small

$$A = \frac{\lambda_2 - \lambda_3}{\lambda_2 + \lambda_3}$$

⇨ Complementary to Entropy H
⇨ Additional discrimination when H > 0.7

Refinement 2: Rotation Angle Correction of Polarimetric Signatures

- **Scattering matrix for even-bounce scatterers:**
  - **If scatterer oriented parallel to flight track:**

$$[S] = \begin{bmatrix} 1 & 0 \\ 0 & -1 \end{bmatrix} \begin{bmatrix} 1 & 0 \\ 0 & e^{i\varphi} \end{bmatrix} \begin{bmatrix} R_{SS} & 0 \\ 0 & R_{PS} \end{bmatrix} \begin{bmatrix} R_{ST} & 0 \\ 0 & R_{PT} \end{bmatrix} = \begin{bmatrix} R_{SS}R_{ST} & 0 \\ 0 & -R_{PS}R_{PT}e^{i\varphi} \end{bmatrix}$$

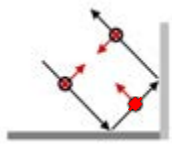

  - **In case of rotation with angle ϕ:**

$$[S] = \begin{bmatrix} \cos(2\phi) & \sin(2\phi) \\ \sin(2\phi) & -\cos(2\phi) \end{bmatrix} \begin{bmatrix} 1 & 0 \\ 0 & e^{i\varphi} \end{bmatrix} \begin{bmatrix} R_{SS} & 0 \\ 0 & R_{PS} \end{bmatrix} \begin{bmatrix} R_{ST} & 0 \\ 0 & R_{PT} \end{bmatrix} = \begin{bmatrix} \cos(2\phi)R_{SS}R_{ST} & \sin(2\phi)R_{PS}R_{PT}e^{i\varphi} \\ \sin(2\phi)R_{SS}R_{ST} & \cos(2\phi)R_{PS}R_{PT}e^{i\varphi} \end{bmatrix}$$

Rotation of dihedral scatterers makes dihedrals look like volume scatterers

Refinement 2: Rotation Angle Correction of Polarimetric Signatures

- **Correction of Rotation Based on Deorientation Concept of Huygens**
  - Minimization of cross-polarized HV component

$$[T] = \begin{bmatrix} T_{11} & T_{12} & T_{13} \\ T_{21} & T_{22} & T_{23} \\ T_{31} & T_{32} & T_{33} \end{bmatrix} \qquad [T(\phi)] = [R_y(\phi)][T][R_y(\phi)]^{-1} \qquad [T(\phi)] = \begin{bmatrix} T_{11}(\phi) & T_{12}(\phi) & T_{13}(\phi) \\ T_{21}(\phi) & T_{22}(\phi) & T_{23}(\phi) \\ T_{31}(\phi) & T_{32}(\phi) & T_{33}(\phi) \end{bmatrix}$$

Equals minimization of T_{33} term in $T(\theta)$: $\quad T_{33}(\phi) = T_{33}\cos^2(2\phi) - \mathrm{Re}\{T_{23}\}\sin(4\phi) + T_{22}\sin^2(2\phi)$

- Minimum found from $T_{33}(\phi) = 0$

Yamaguchi, Y., Sato, A., Boerner, W.-M., Sato, R., Yamada, H., "Four-Component Scattering Power Decomposition With Rotation of Coherency Matrix," IEEE TGRS, 10:55, pp. 1-8, 2011

Before Rotation Angle Correction

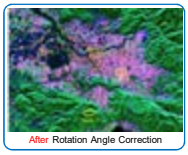

After Rotation Angle Correction

Fugen-dake Unzen
32.825N; 130.364E; 2007/6/5
ALPSRP072570650-1.1A

T_{33} Rotation
Scattering power decomposition
Pd, Pv, Ps

Pauli-basis
HH-VV, 2HV, HH+VV

Sinclair-basis
HH, 2HV, VV

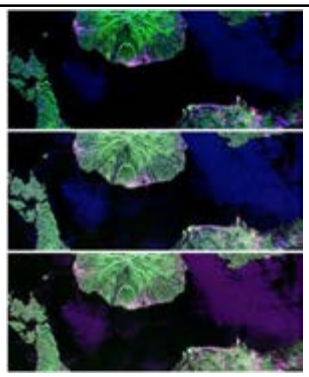

37

Iwate-San Morioka Iwate
39.747N 140.976E; 2007/3/28
ALPSRP062500790-1.1A

T_{33} Rotation
Scattering power decomposition
Pd, Pv, Ps

Pauli-basis
HH-VV, 2HV, HH+VV

Sinclair-basis
HH, 2HV, VV

38

Bangladesh
21.923N 89.904E; 2009/04/08
ALPSRP224000430

T_{33} Rotation
Scattering power decomposition
Pd, Pv, Ps

Pauli-basis
HH-VV, 2HV, HH+VV

Sinclair-basis
HH, 2HV, VV

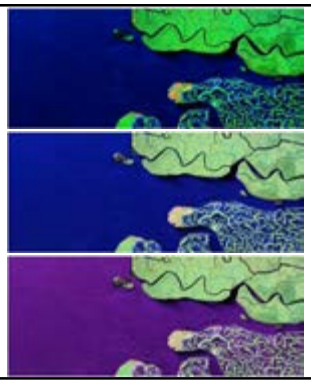

39

Available Software Tools

- **PolSARPro is a freely available software tool provided by ESA**
- Can be downloaded at: https://earth.esa.int/web/polsarpro/home
- It includes all available polarimetric decomposition methods for dual-pol and quad-pol SAR data
- In addition to the software also tutorials to Polarimetry can be downloaded
- Includes polarimetric analysis of Sentinel-1 dual-pol data

EXAMPLES OF SAR IMAGE CLASSIFICATION

The H / α Classifier

Example Natural Environment

- **Mixed natural environment in Germany**

Optical image

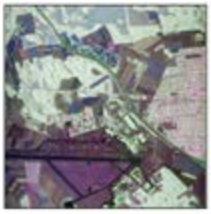

Polarimetric SAR color composite

The H / α Classifier
Example Natural Environment

- **Mixed natural environment in Germany**

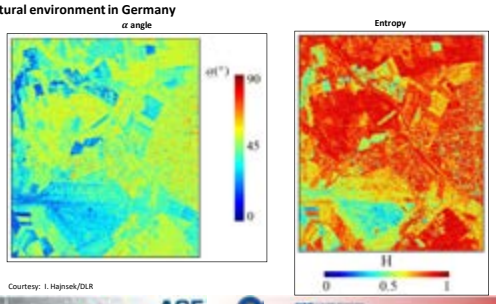

Courtesy: I. Hajnsek/DLR

The H / α Classifier
Example Natural Environment

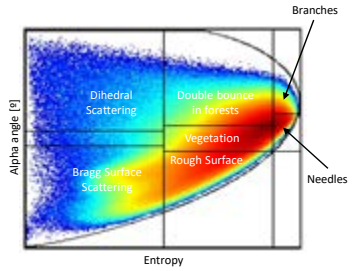

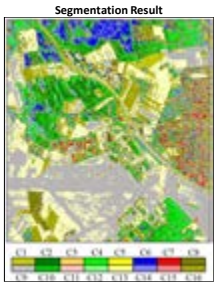

Courtesy: I. Hajnsek/DLR

The H / α Classifier
Example: San Francisco Bay Area

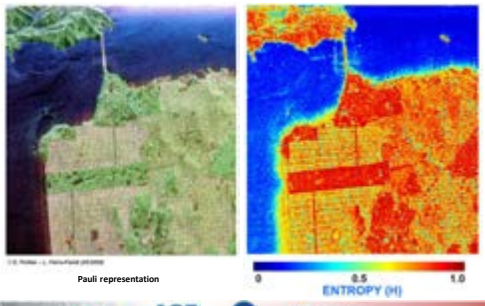

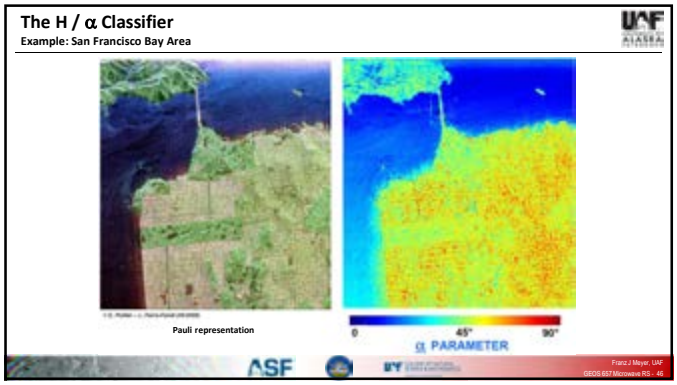
The H / α Classifier
Example: San Francisco Bay Area
Pauli representation
0
45°
90°
α PARAMETER
ASF
Franz J Meyer, UAF
GEOS 657 Microwave RS - 46

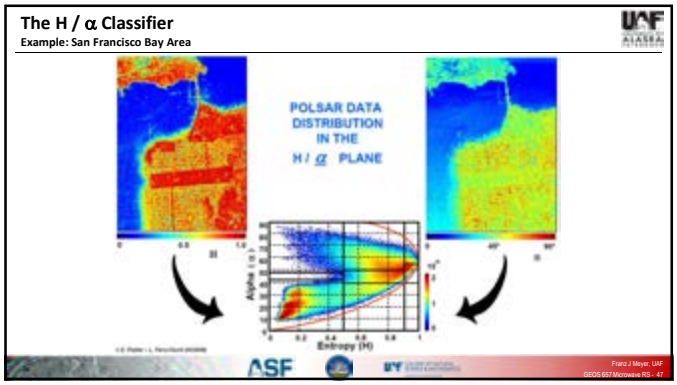
The H / α Classifier
Example: San Francisco Bay Area
POLSAR DATA
DISTRIBUTION
IN THE
H / α PLANE
Alpha (α)
Entropy (H)
ASF
Franz J Meyer, UAF
GEOS 657 Microwave RS - 47

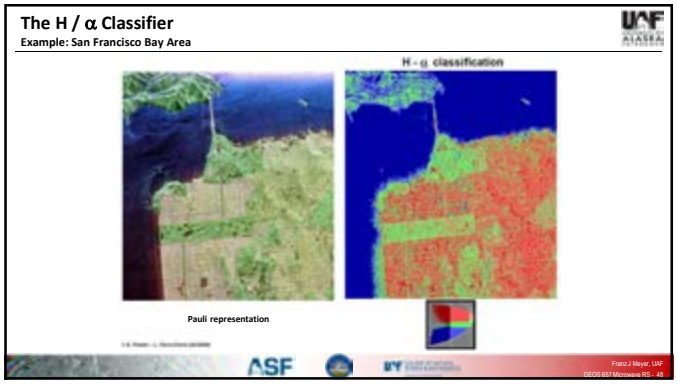
The H / α Classifier
Example: San Francisco Bay Area
H - α classification
Pauli representation
ASF
Franz J Meyer, UAF
GEOS 657 Microwave RS - 48

The H / A / α Classifier

Example: San Francisco Bay Area

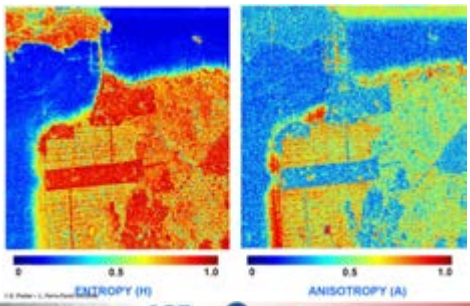

Unsupervised Classification based on the H / A / α Decomposition

- **Disadvantage of H / A / α classification schemes:**
  - H / α classification space is sub-devided into 9 basic zones
  - Location of the boundaries is fairly arbitrary and generic
  - Therefore, H / A / α classification is not optimal and more advanced ways for determining class boundaries are sought.
- **Solution:**
  - In newer approaches H / A / α classification results are combined with a subsequent Wishart or maximum likelihood classification to improve performance.
  - H / A / α classification results provide initial class centers that are improved in subsequent classification

Unsupervised Classification based on the H / A / α Decomposition

- **Example of k-mean classification procedure:**

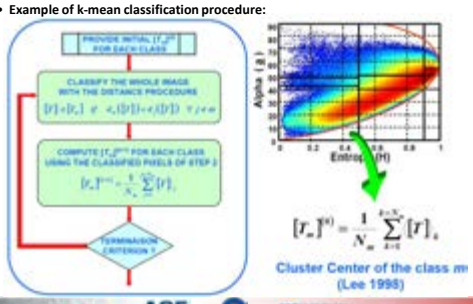

$$[T_m]^{(k)} = \frac{1}{N_m} \sum_{k=1}^{k=N_m} [T]_k$$

Cluster Center of the class m
(Lee 1998)

Unsupervised Classification based on the H / A / α Decomposition

- Example of k-mean classification procedure:

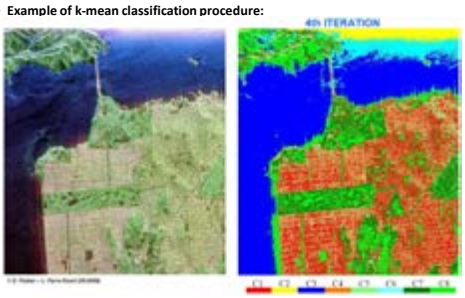

Unsupervised Classification based on the H / A / α Decomposition

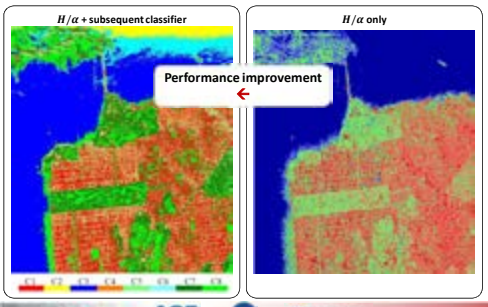

Polarimetric Classification

The Role of the Observation Frequency

- Different penetration in different frequencies produce different polarimetric signatures

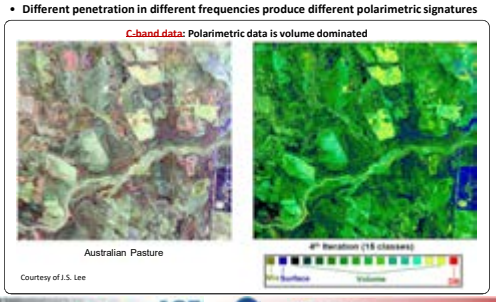

Polarimetric Classification

The Role of the Observation Frequency

- **Different penetration in different frequencies produce different polarimetric signatures**

L-band data: Higher penetration causes more surface signal

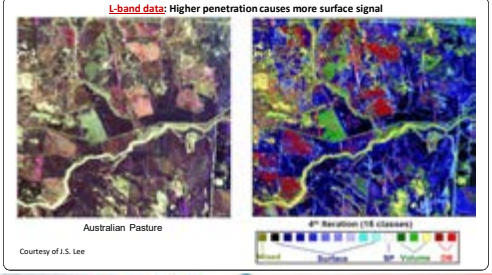

Courtesy of J.S. Lee

What's Next?

- **Next lecture** we will talk about SAR Interferometry (InSAR).

- **In preparation for this lecture please read the following pages in Woodhouse (2006):**
  - Pages 312-331: Radar Interferometry